MAGNETIC ANOMALIES OVER PERMANENTLY SHADOWED CRATERS NEAR THE LUNAR SOUTH POLE: MAPPING AND IMPLICATIONS. L. L. Hood, I. Bryant, and J. van der Leeuw, Lunar and Planetary Laboratory, University of Arizona, Tucson, Arizona, 85721, USA, lon@lpl.arizona.edu

Introduction: As reviewed recently by Lucey et al. [1], potential contributors of volatiles to the lunar surface include the solar wind ion bombardment, volatile-rich impactors, and interior outgassing. In particular, solar wind hydrogen can react with lunar oxygen to form hydroxyl [2]. On the other hand, solar wind ion sputtering is one of several non-negligible loss mechanisms for water ice in permanently shadowed regions (PSRs) near the lunar poles (e.g., [3]). The surface abundance of hydroxyl is observed to be reduced in areas with strong surface magnetic fields (swirls), which deflect the ion bombardment [4].

Previous estimates of the solar wind hydrogen flux onto the surfaces of lunar south polar craters have considered only the ambient solar wind flow and effects of topography [5]. Previous mapping has shown evidence for non-negligible magnetic anomalies over the south polar region (e.g., [6]). Because of the low angle of solar wind incidence near the lunar poles, even moderate magnetic anomalies may significantly deflect the ion bombardment [7]. It is therefore important to map crustal fields in this area as accurately as possible and determine whether anomalies exist over PSRs. Here, we apply a newly developed technique [8], which more accurately maps the amplitudes and shapes of weaker anomalies.

Mapping: The mapping method consists of first constructing regional maps of improved accuracy over individual areas by selecting only the best magnetometer measurements (lowest altitude with least amount of external field contamination) over those specific areas. Once the best measurements are identified, an equivalent source dipole (ESD) technique (e.g., [9]) can be applied to normalize the measurements to a constant altitude. Individual regional maps can then be joined together to produce a larger-scale map. A large-scale map of the crustal field has recently been constructed using this approach at 30 km altitude covering latitudes from 65°S to 65°N [8]. Interpretation of the map supports the hypothesis that many lunar magnetic anomaly sources consist of impact basin ejecta that is enriched in iron from the impactor.

Figure 1 shows a map of the field magnitude in the southern hemisphere (50°S to the pole) at 30 km altitude produced using the new methodology. Magnetometer data from the Kaguya (KG) mission in 2009 ([6] and references therein) were employed because it had excellent low-altitude coverage under relatively quiet external field conditions. The contour interval is 1 nT.

To produce the complete map, 12 overlapping regional maps, each covering 40° of longitude and 40° of latitude (50°S to the pole), were first constructed in a series of steps. The first step was to examine all available KG orbit segments to select only the best measurements over each of the 12 regions. This eliminated short-term field fluctuations of external origin. To minimize longer wavelength external fields, quadratic detrending was applied. Then the measurements were effectively normalized to a common altitude using an equivalent source dipole technique as described in [8]. Finally, the 12 regional maps were joined together followed by two-dimensional filtering to produce an effective horizontal resolution of about 75 km (~2.5° in latitude).

In addition to anomalies at southern mid-latitudes (50°S to 65°S) described earlier [8], a cluster of anomalies with smoothed amplitudes exceeding 2 nT is present near the south pole.

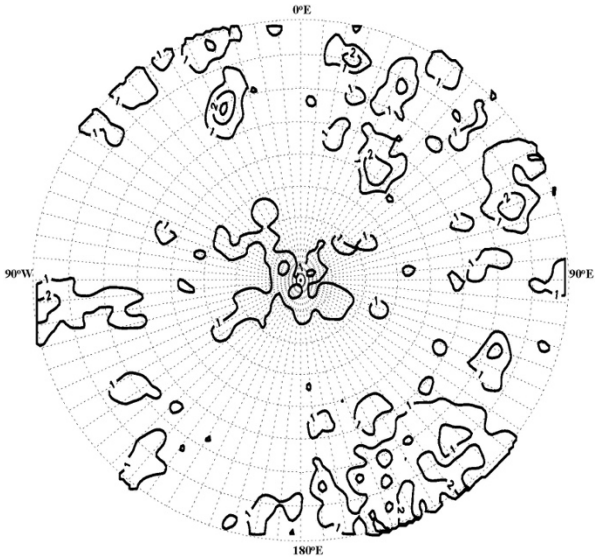

Figure 1

The South Polar Anomaly Group: The best prior map of the near-polar region is that of Tsunakawa et al. [6] at 30 km altitude. Figure 2a below superposes their map at this altitude onto a topographic map [10] of the region. Figure 2b superposes the map of Figure 1 (also at 30 km altitude) onto the same area to allow a direct comparison. While the map of Figure 2a agrees qualitatively with that of Figure 2b, there are differences in detail which we believe are better mapped in Figure 2b.

The available KG magnetometer data over the south polar region were obtained at relatively low altitudes (as low as 15 km above the mean lunar radius). It is therefore possible to apply the ESD solution to construct a map at a lower altitude than 30 km. Figure 2c is an alternate map evaluated at a constant altitude of 20 km. It is similar to that of Figure 2a but the anomaly amplitudes are larger. In particular, relatively strong anomalies are directly over several permanently shadowed craters including Shoemaker and Sverdrup.

Discussion and Conclusions: Moderate magnetic anomalies are present directly over at least two permanently shadowed craters near the lunar south pole. While these anomalies (and lunar magnetic anomalies in general) are too weak to shield future astronauts from biologically harmful cosmic radiation, they could assist in shielding these craters and any water ice therein from the solar wind ion bombardment.

Filtered anomaly amplitudes at 30 km altitude are ~2 nT, smaller than the amplitudes of the strongest lunar anomalies that are known to strongly deflect the ion bombardment (e.g., ~ 8 nT for the Reiner Gamma anomaly filtered to the same resolution; Figure 5 of [8]). However, as noted above, the very low angle of incidence of the ion bombardment near the lunar poles could nevertheless make these anomalies very effective in reducing the ion flux in the surfaces of PSRs. Field amplitudes at the surface could easily exceed 100 nT. Future estimates of the solar wind hydrogen flux within permanently shadowed craters should therefore consider deflection by crustal fields in addition to the ambient plasma flow and effects of topography.

Acknowledgments: Supported under a grant from the NASA LDAP program (80NSSC21K1478). Kaguya (SELENE) vector magnetometer data are available from the Japan Aerospace Exploration Agency at http://darts.isas.jaxa.jp/planet/pdap/selene.

References: [1] Lucey, P. G. et al. (2022) *Geochemistry*, in press; doi:10.1016/j.chemer.2021.125858 [2] Zeller, E. J. et al. (1966) *J. Geophys. Res.*, *71*, 4855-4860. [3] Zimmerman, M. I. et al. (2011) *GRL, 38,* No. 2548. [4] Kramer, G. Y. et al. (2011) *J. Geophys. Res. Planets, 116*, E00G18, doi:10.1029/2010JE003729. [5] Rhodes, D. J. & W. M. Farrell (2020), *Planet. Sci. J., 1:13* (8 pp), doi:10.3847/PSJ/ab8939 [6] Tsunakawa H. et al. (2015) *JGR Planets, 120,* 1160-1185. [7] Hood, L. L. & C. Williams (1989), *Proc. Lunar Planet. Sci. Conf. 19th*, 99-113. [8] Hood L. L. et al. (2021) *JGR Planets, 126,* doi: 10.1029/2020JE006667. [9] Hood, L. L. (2015) *GRL, 42,* 10,565-10,572, doi:10.1002/2015GL066451 [10] Stopar, J. & H. Meyer (2019), *Topographic Map of the Moon's South Pole (80°S to Pole),* LPI Contribution 2169, ht*tps://repository.hou.usra.edu/handle/20.500.11753/1254.*

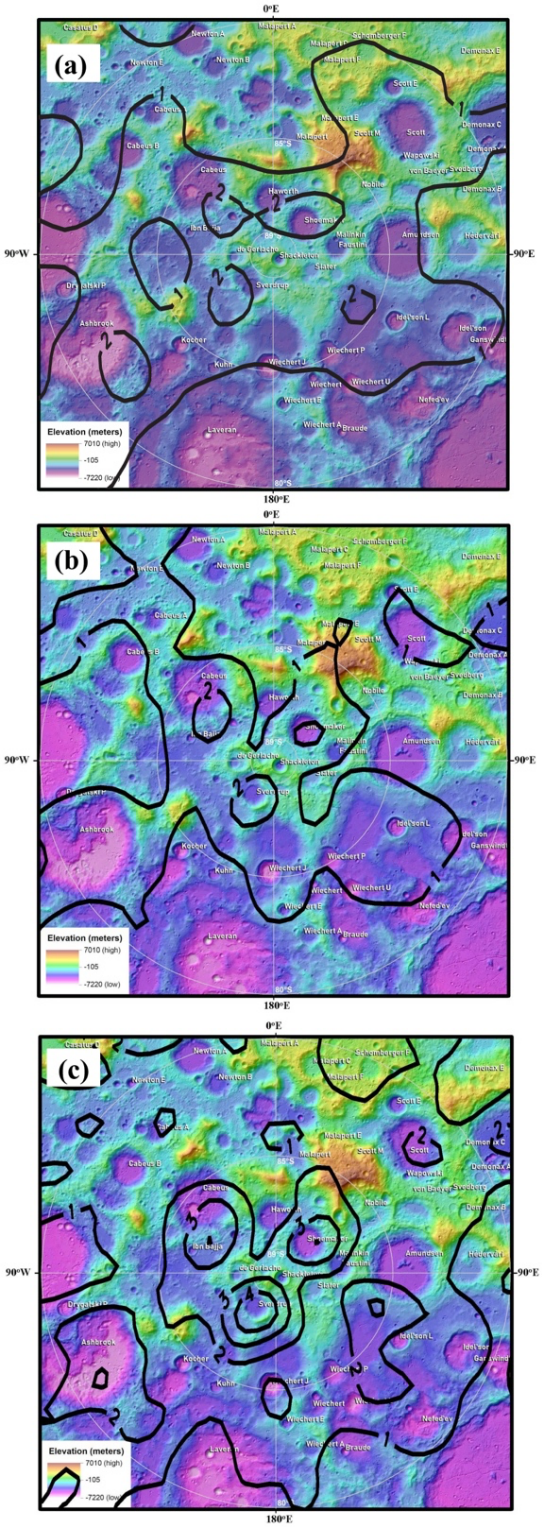

Figure 2